School of Mathematics
Trinity College Dublin

String Tension of Quark-Anti-Quark Pairs in Lattice QCD

Author:
David Taylor

Supervisor:
Prof. Mike Peardon

Abstract

This project used lattice QCD gauge field configurations to measure the energy of a static quark-anti-quark pair for various separations. String tensions for several different pion masses were obtained. The string tensions and Coulomb parameters were plotted against the respective pion masses. The string tension for a physical π^+ meson was obtained to be $\sqrt{\sigma} = 463.7 \pm 23.7$ MeV, with a Coulomb parameter $\alpha = 0.096 \pm 0.002$.

Acknowledgements

I was given several books by Prof. Peardon, which gave me access to vital information needed to grasp the ideas and concepts of LQCD. He also provided me with sample scripts to run the executables on the HPC machines which was essential in gathering the data. Graduate students Graham Moir, Tim Harris and Pol Vilaseca Mainar also helped a great deal by giving tutorials in the understanding of QCD and QFT in general. I am very grateful for the advice and encouragement I received.

Contents

Chapter 1

Introduction

Quantum Chromodynamics (QCD) is the theory which describes interactions between quarks and gluons via the strong nuclear force. It is a quantum field theory, specifically a non-abelian gauge theory of $SU(3)$. It describes the "color field" which is mediated by gluons.
Gluons, unlike their counterpart photons in QED, are self-interacting. That is, gluons carry color charge. This has a significant outcome; *confinement*.

Confinement is the phenomenon whereby the potential between quarks increases with separation. This is due to gluons carrying, as well as mediating color charge. This leads to quarks being bound in "colorless" states known as hadrons.

The gluon-gluon interactions give rise to producing so called "flux tubes". These are string-like objects which are manifested from the color field. It is this string tension which is of interest here.

1.1 Brief History of QCD

The birth of QCD is not a clear-cut one. There were hints of its emergence by 1965 when Han and Nambu said that QCD is a Yang-Mills theory in which the basic particles are quarks, the gauge group is color $SU(3)$, there are eight gluons which mediate the force and that they carry color charge

[8]. They also noted that hadrons would be colorless. Despite this, QCD was not yet formed. By 1967 the idea of Yang-Mills theory appealed to many, however it was not known whether it was renormalizable. Glashow, Weinberg and Salam had, by this time, set out a Yang-Mills theory of the weak force. Veltman and 't Hooft showed in 1971 that it was renormalizable [9].
This was what was needed to make Yang-Mills theory interesting again. The electroweak theory was resuscitated and there began the natural extension to think of the strong interaction in terms of Yang-Mills theory.

From late 1971, Gell-Mann spent some time working at CERN with Fritzsch and Bardeen from Princeton. Bardeem was concerned with the discrepancy of the decay rate of the neutral pion into two photons. Experiment was nine times the theorized rate. Gell-Mann, Fritzsch and Bardeem wrote a paper in 1972 [10] which showed that the decay rate matched theory and experiment if each of the quarks are assigned three colors. In the same paper they also explained another discrepancy, that of the ratio of hadrons to muons in electron-positron collisions.

Again in 1972, Gell-Mann presented a paper on behalf of himself and Fritzsch at the XVI International Conference on High Energy Physics [11], at the National Accelerator Laboratory (as Fermilab was then known). In this paper, they tried to model the strong interaction with colored quarks, however, they were using a single, colorless gluon. It begins to sound more like QCD, "real particles are required to be singlets with respect to the $SU(3)$ of color". They also referred to the idea that gluons too should be colored. "For example, they could form a color octet of neutral vector fields obeying the Yang-Mills equations,". This paper to some is the birth of QCD.

A third result further pushes toward QCD. in 1969, it was shown at SLAC that protons seemed to contain point-like scattering centres. This was a major challenge for theorists. It was shown by Gross, Wilczek and Politzer that at high energies, the interaction strength for Yang-Mills theory decreases to nothing. They noted "one can construct many interesting models of the strong interaction", one being where quarks having the same flavour but different colors are mixed by virtue of neutral "vector mesons"; gluons. This sounds more like QCD. In fact, Gross claims that he and Wilczek were the first to publish the master equation of QCD.

1.2 Moving to LQCD

The problem with QCD is that for low energies, the coupling parameter is extremely high; so much so that perturbative methods fail. Wilson introduced, in 1974 the idea of discretizing spacetime and putting it on a lattice [12] which allows the infinities that emerge from QCD to be controlled. In the limit of the distance between the points shrinking to zero and the volume growing to infinity, the continuum is recovered.

The four-dimensional lattice is represented by sets of numbers in a computer, but is analogous to the more familiar two and three dimensional lattices. The points on the lattice represent the quarks and the links represent the gluons. A typical number of lattice points to consider would be 48 in each dimension; this leads to $48^4 = 5,308,416$ lattice points in all. This is equivalent to calculating the volume of an irregular region within a box having almost two hundred million sides [13].

This problem is dealt with by using a Monte Carlo sampling estimation method to calculate the path integral. In practice, to calculate the mass of, say, a π^+, a number of lattice points for the four dimensions, quark masses and interaction strength are fed into a computer. Then an initial configuration is introduced. The Monte Carlo program creates several hundred independent configurations based on the initial one. The probability that the up and anti-down quarks (i.e. the π^+) can propagate along the time dimension of the lattice can be computed from the average values of each of the configurations of the quark, anti-quark and gluon fields.

Since the distance a particle will propagate through the lattice falls away with mass and temporal spacing, the decay rate in the particle making its journey can be used to determine a value for its mass.

1.3 Approach

Feynmann showed the equivalence of the path integral formulation to the partition function formulation. Thus, to calculate correlation functions, a solution to equation 1.1 is needed.

$$\mathcal{Z} = \int_{\psi,\mathcal{A}} d\psi d\mathcal{A} e^{iS} \iff \mathcal{Z} = \mathrm{Tr}[e^{-\hat{H}T}] \tag{1.1}$$

Where S is the action and $\hat{H}$ is the Hamiltonian.
However, this is infinite dimensional over the fields ψ and $\mathcal{A}$. We must therefore consider approximate solutions. The natural choice would be perturbation theory which is the approach used in quantum electrodynamics (QED). The perturbation method works only if the coupling constant g is much less than 1. This is the case in QED, but not in QCD, where $g > 1$. Another method is needed.

Lattice QCD (LQCD) is a non-perturbative approach to solving this problem. It is a lattice gauge theory which places quarks on the sites of the lattice and gluons on the connecting links. LQCD discretizes four-dimensional spacetime into four-dimensional Euclidean space.
Two immediate problems are that of lattice spacing and finite boundary. The volume of the lattice should ideally be infinite and the lattice spacing should be close to zero. As mentioned above in the limit of infinite volume and zero lattice spacing, the continuum is recovered.

The lattice formulation is suited to parallel processing as a regular lattice can be distributed evenly on a four-dimensional physical network among parallel nodes [7].

1.3.1 Outline of Steps Involved in LQCD

1. Perform the Wick rotation, mapping Minkowski spacetime to Euclidean space.

2. Discretize the Euclidean action.

3. Then the operators in the correlation functions become classical field variables.

4. Compute the correlation functions on a given lattice configuration, using the Boltzmann e^{-S} factor as a weight.

Chapter 2

Theory

2.1 Correlation Function

Consider a finite number of sites on a one-dimensional lattice. The two-point *correlation function* is defined as follows [1]:

$$C(t_2, t_1) = \langle 0|\hat{\Phi}(t_2)\hat{\Phi}^\dagger(t_1)|0\rangle_T \tag{2.1}$$

Setting $t_1 = 0$ and $t_2 = t$, we have

$$C(t) = \langle 0|\hat{\Phi}(t)\hat{\Phi}^\dagger(0)|0\rangle_T \tag{2.2}$$

where $\hat{\Phi}(t)$ is a quantum mechanical operator acting on a hilbert space and T is temperature. In particular, the operator (and Hermitian conjugate) is given in the Heisenberg representation by,

$$\hat{\Phi}(t) = e^{i\hat{H}t}\hat{\Phi}e^{-i\hat{H}t}, \qquad \hat{\Phi}^\dagger(t) = e^{-i\hat{H}t}\hat{\Phi}^\dagger e^{i\hat{H}t} \tag{2.3}$$

with $\hbar = 1$.

2.2 Wick Rotation

In order to calculate quantities such as the mass or the string tension numerically, we must transform from a *Minkowski* space-time to a *Euclidean* space. We make the following transformation to imaginary time, i.e. a Wick Rotation.

$$t \mapsto -i\tau \tag{2.4}$$

which gives,

$$\hat{\Phi}(\tau) = e^{\hat{H}\tau}\hat{\Phi}e^{-\hat{H}\tau}, \qquad \hat{\Phi}^\dagger(\tau) = e^{-\hat{H}\tau}\hat{\Phi}^\dagger e^{\hat{H}\tau} \tag{2.5}$$

so the correlation function becomes,

$$C(\tau) = \langle 0|e^{-\hat{H}(T-\tau)}\hat{\Phi}e^{-\hat{H}\tau}\hat{\Phi}^\dagger|0\rangle_T \tag{2.6}$$

2.3 Quark Fields on the Lattice

Consider a finite lattice of N sites with periodic boundary conditions. Applying a creation operator at $\hat{\Phi}^\dagger(0)$ and an annihilation operator at $\hat{\Phi}(\tau)$ and inserting a complete set of eigenstates, the correlation function may be written as follows [1]:

$$\begin{aligned} C(\tau) &= \langle \hat{\Phi}(\tau)\hat{\Phi}^\dagger(0)\rangle_T \\ &= \frac{1}{\mathcal{Z}(T)}\sum_{m,n}\langle m|e^{-\hat{H}(T-\tau)}\hat{\Phi}|n\rangle\langle n|e^{-\hat{H}\tau}\hat{\Phi}^\dagger|m\rangle \end{aligned} \tag{2.7}$$

where $\mathcal{Z}(T)$ is the partition function and is given by

$$\begin{aligned} \mathcal{Z}(T) &= \sum_n \langle n|e^{-\hat{H}T}|n\rangle \\ &= \mathrm{Tr}[e^{-\hat{H}T}] \end{aligned} \tag{2.8}$$

By using the eigenvalue equation, the completeness and normalization relations:

$$\hat{H}|n\rangle = E_n|n\rangle, \qquad \mathbb{1} = \sum_n |n\rangle\langle n|, \qquad \langle n|n\rangle = 1 \tag{2.9}$$

we then have

$$C(\tau) = \frac{1}{\mathcal{Z}(T)} \sum_{m,n} \langle m|\hat{\Phi}|n\rangle\langle n|\hat{\Phi}^{\dagger}|m\rangle e^{-E_m(T-\tau)} e^{-E_n\tau} \tag{2.10}$$

Using equation 2.9, 2.8 becomes

$$\begin{aligned} \mathcal{Z}(T) &= \sum_n e^{-E_nT} \\ &= e^{-E_0T} + e^{-E_1T} + e^{-E_2T} + \cdots \end{aligned} \tag{2.11}$$

Defining the difference in energy from the vacuum state as

$$\Delta E_n = E_n - E_0 \tag{2.12}$$

then the partition function becomes

$$\mathcal{Z}(T) = e^{-E_0T}(1 + e^{-\Delta E_1T} + e^{-\Delta E_2T} + \cdots) \tag{2.13}$$

Subbing this into equation 2.10 we get,

$$C(\tau) = \frac{\sum_{m,n} \langle m|\hat{\Phi}|n\rangle\langle n|\hat{\Phi}^{\dagger}|m\rangle e^{-\Delta E_n\tau} e^{-\Delta E_m(T-\tau)}}{1 + e^{-\Delta E_1T} + e^{-\Delta E_2T} + \cdots} \tag{2.14}$$

Thus, the correlation function depends on the energies normalized relative to the vacuum energy E_0. So denote ΔE_n by E_n

Now we take the limit as $T \to \infty$

$$\lim_{T\to\infty} C(\tau) = \lim_{T\to\infty} \frac{\sum_{m,n} \langle m|\hat{\Phi}|n\rangle\langle n|\hat{\Phi}^{\dagger}|m\rangle e^{-E_n\tau} e^{-E_m(T-\tau)}}{1 + e^{-E_1T} + e^{-E_2T} + \cdots} \tag{2.15}$$

The sum of the exponentials in the denominator tends to 0 thus leaving 1. Similarly, in the numerator only the $E_m = 0$ terms survive the limit, so we get

$$
\begin{aligned}
\lim_{T\to\infty} C(\tau) &= \sum_n \langle 0|\hat{\Phi}|n\rangle\langle n|\hat{\Phi}^\dagger|0\rangle e^{-E_n\tau} \\
&= |\langle n|\hat{\Phi}^\dagger|0\rangle|^2 e^{-E_n\tau} + |\langle n'|\hat{\Phi}^\dagger|0\rangle|^2 e^{-E_{n'}\tau} + \cdots
\end{aligned}
\tag{2.16}
$$

where n, n' etc. are the excited states. So we have that the correlation function is exponentially decreasing.

2.3.1 Choosing Operators

From equation 2.16, it is clear that the energy does not depend on the coefficients. Thus, to measure the energy more easily, these coefficients are chosen to be as large as possible. These are the smearing values discussed below. The energy E_n is the *string tension* i.e. $\sqrt{\sigma}$.

2.4 Potential Between Static Quarks

If a quark-anti-quark pair are forced apart, the potential between them increases linearly with separation [2]. As the pair become more and more separated there comes a point where the potential becomes large enough to create another quark anti-quark pair. This effect is due to confinement which is due to the color charge.

It seems that only colorless combinations of quarks are observable. E.g. a proton is observable since its three quarks (two up and one down) are combined in a colorless state. In a quark-anti-quark pair, where again the composite meson is colorless, as the pair are separated, the string tension becomes larger and larger; at some point it becomes more favourable for another quark-anti-quark pair to form than for the string tension to further increase.

Thus, it would seem that quarks may not be observed individually, that is they respect the color symmetry.

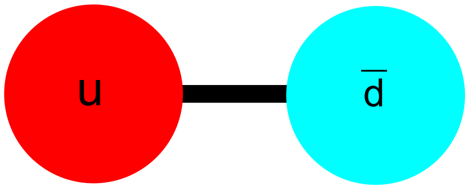

Figure 2.1: A pion-plus, π^+, quark-anti-quark pair. A red up and anti-red anti-down connected by a gluon.

2.4.1 Wilson Loop

Consider a static pair of charges created at imaginary time τ_1 and annihilated at τ_2. This is the correlation function from section 2.1. This construct is known as a *Wilson Loop* [3].

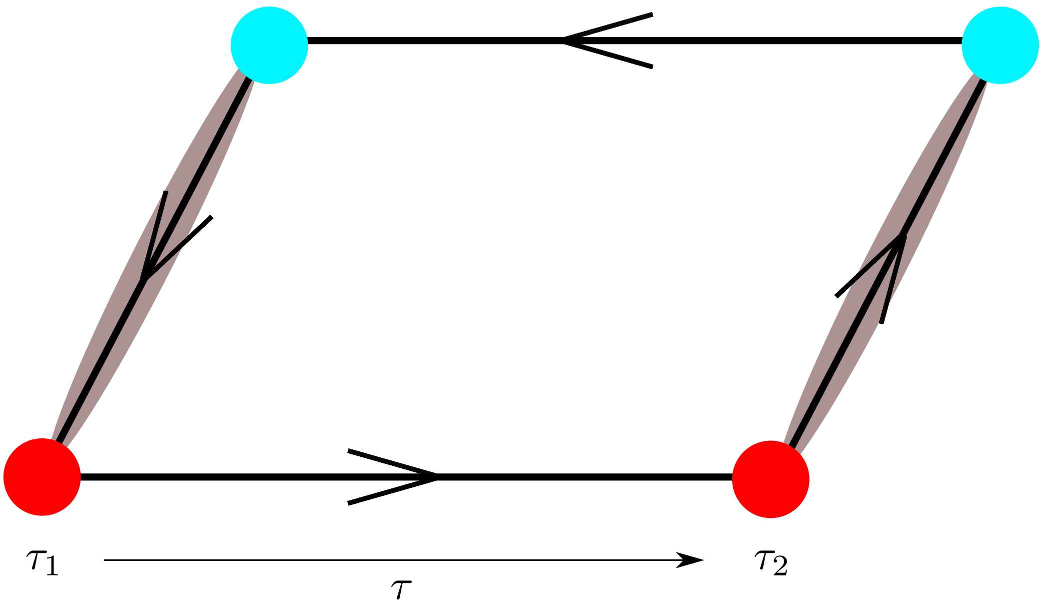

Figure 2.2: A graphical representation of a Wilson loop for a π^+ created at τ_1 and annihilated at τ_2. It is the measurement of the exponential decay of this propagator that gives the string tension.
Shown also, is the gluon flux tube connecting the quark and anti-quark.

Chapter 3

Smearing Optimization

To determine which values for the smear file were best, a range of values were tested using the following method [5].

3.1 Method

Firstly, various smearing configurations ranging from 0.1 to 0.8 with 5 iterations were chosen. Then for each of these smearings, the R3 separation was found and plotted, figure 3.1.

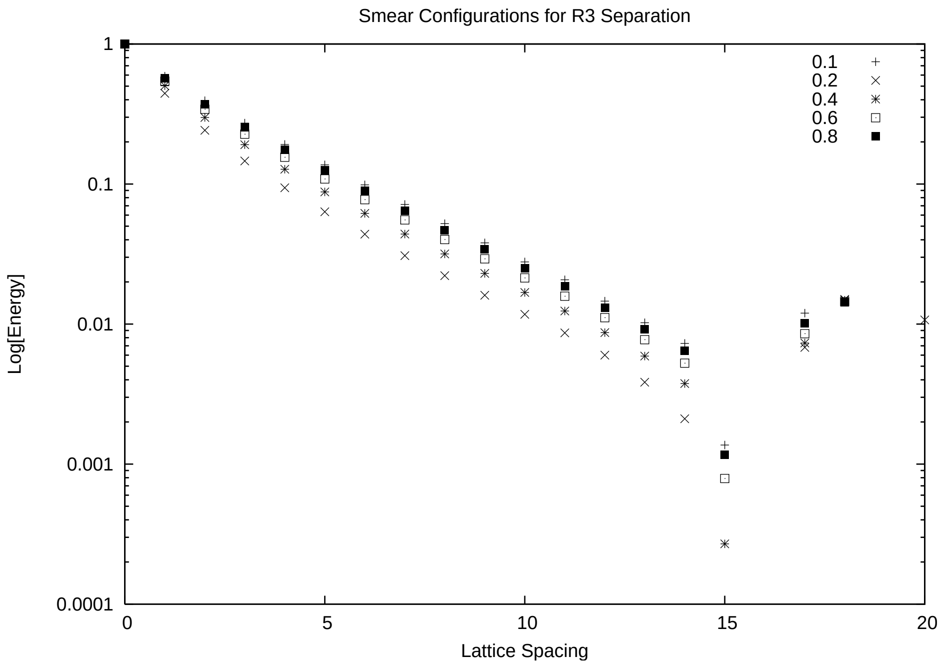

Figure 3.1: Configurations with 5 iterations.

It should be noted that the log plots for the various smearings give parallel lines as a good fit. This implies, as expected, that the string tension is unaffected by the smearing configurations.

Further testing was done over the same range of values, but for 10 iterations, figure 3.2.

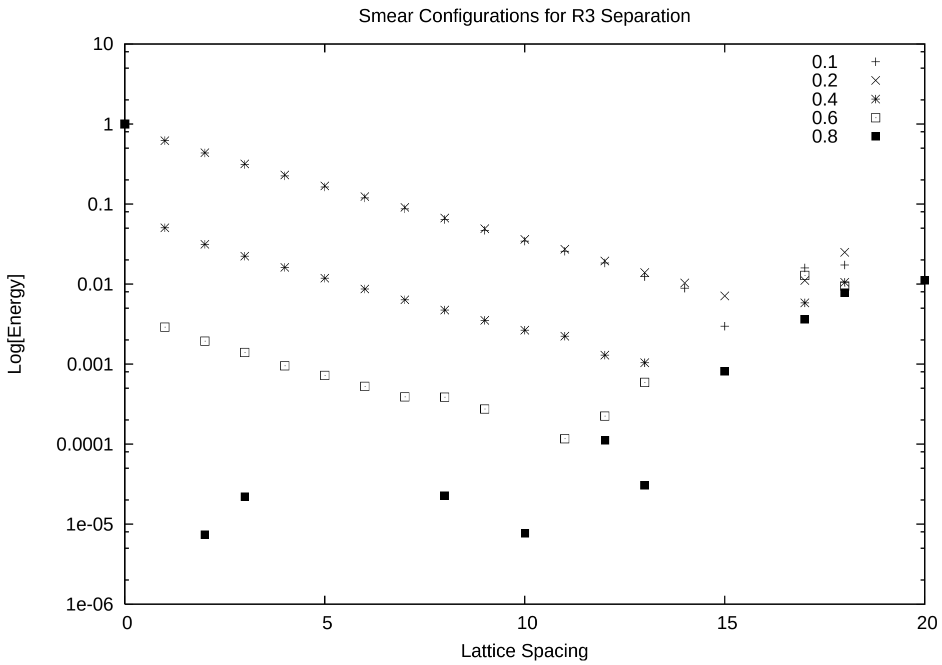

Figure 3.2: configurations with 10 iterations.

Again, as expected, the string tension is unaffected by the smearing configurations.

3.2 Further Testing

More values were then tested.

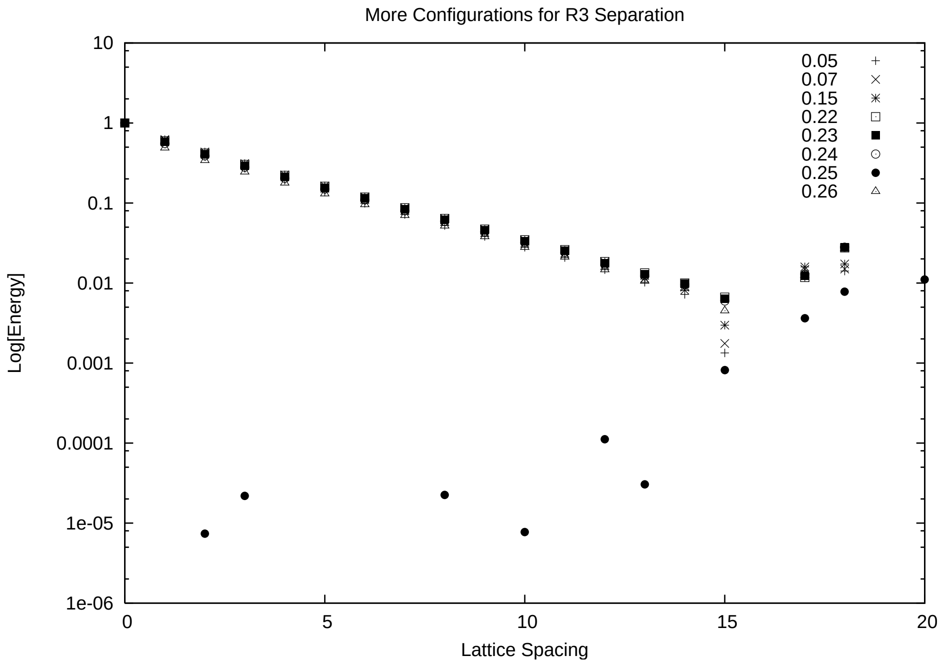

Figure 3.3: more configurations with 10 iterations.

The data becomes *noisy* for the value 0.25, so the 0.24 value was chosen to be used for the second, third and fourth datasets.

Chapter 4

First Dataset

This first dataset was a trial run of the procedure, which followed in the later datasets. Thus, these configurations did not contain any quark fields and so the results are not used in the final analysis.

A simple script was run for various gauge field configurations [6] over a range of separations. This returned datasets which were then concatenated and imported into *Mathematica* where it was analysed as follows:

- The data was of the form where each gauge configuration was performed over the twenty separations. Various functions in *Mathematica* were defined to simplify the handling of the data.
- The average value over all the configurations for each separation was evaluated and then plotted, figure 4.1.
- Appropriate mass values were determined for each separation and plotted against lattice spacing 4.2.
- A Cornell fit was applied and the string tension was extracted.

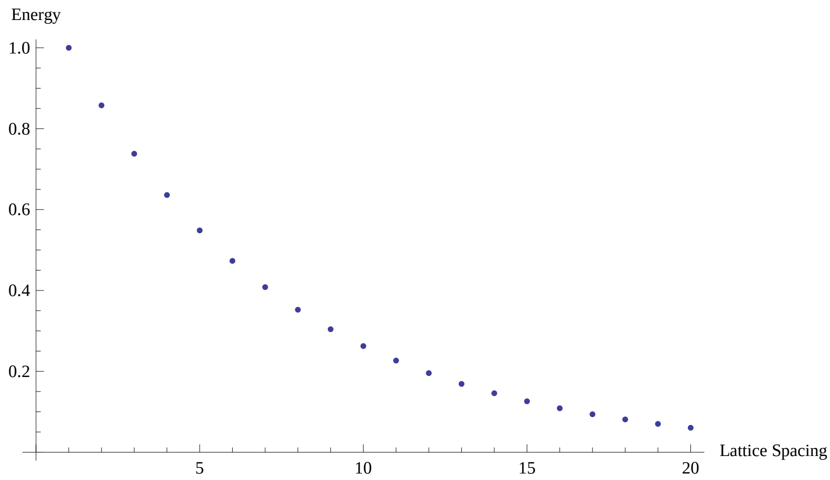

Figure 4.1: Energies over 20 temporal separations for 1 spacial separation.

This is what would be expected, i.e. an exponentially decreasing correlation function.

The log plot of this gives a straight line with negative slope. It is the negative of this slope that we wish to determine; it is the *string tension*. The negative slope for each log plot was found and these values were plotted.

A Cornell fit was applied; equation 4.1. *Gnuplot* was used to determine the fit parameters and to produce the final plot.

$$V(r) = V_0 - \frac{\alpha}{r} + \sigma r \tag{4.1}$$

A value for string tension was found to be $\sqrt{\sigma} = 549.8$MeV, which is reasonable.

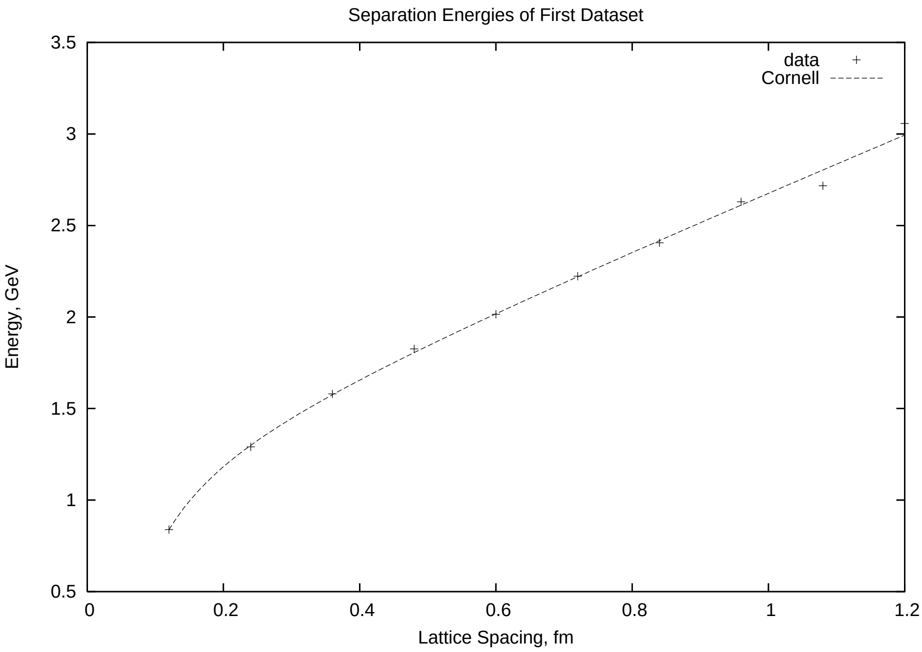

Figure 4.2: Figure showing the string tension $\sqrt{\sigma} = 549.8\text{MeV}$

Chapter 5

Second Dataset

This dataset contained many more gauge configurations [6] than the first. The same procedure was followed and the correlation functions displayed exponential decay.

For this dataset, a second script was used to determine the *best fit* via the χ^2 method. This script ran over ranges of values for t_{max} and t_{min}. The resulting output files gave values of the best fit in terms of χ^2. It also gave the corresponding masses and errors along with the fit ranges. These files were then concatenated and imported into *Mathematica* where they were analysed.

5.1 First Approximation

As a first approximation, the minimum of the quotient of the set of χ^2 values and the set of degrees of freedom was computed. The corresponding mass values and errors were then found. This was done for all separations. These masses were then plotted and a Cornell fit was used, figure 5.1. A string tension of $\sqrt{\sigma} = 504 \pm 26$MeV was found.

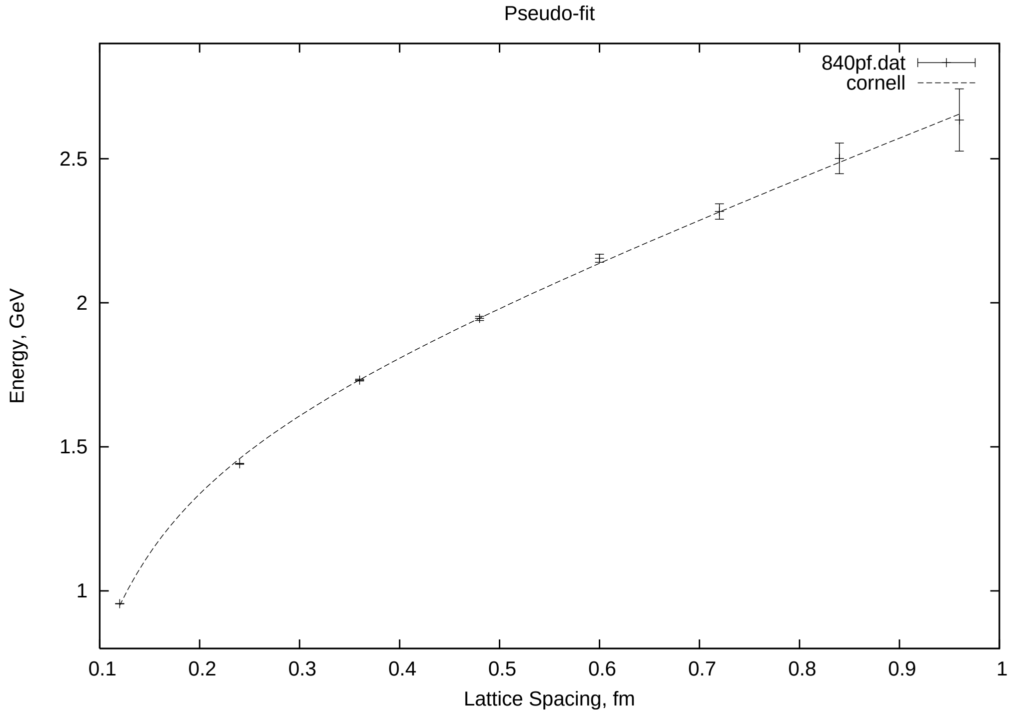

Figure 5.1: $\sqrt{\sigma} = 504 \pm 26\text{MeV}$
This is a good first approximation.

5.2 Goodness of Fit function

As a more accurate method of choosing the correct mass value, several functions from *Numerical Recipes in C* were used [4].

Firstly, a function to determine the probability that a particular value of χ^2 should occur by chance was found to be:

$$Q(N, \chi^2) = \frac{1}{\Gamma(N)} \int_{\chi^2}^{\infty} e^{-t} t^{N-1} dt, \qquad N > 0 \tag{5.1}$$

where N is the number of degrees of freedom.

This formula led to some irregularities. Namely, it gave some *negative* probabilities (perhaps due to "rounding errors" in *Mathematica*). This was rectified by evaluating the indefinite integral and then evaluating the limits to get,

$$Q(N, \chi^2) = \frac{\Gamma(N/2, \chi^2/2)}{\Gamma(N/2)} \tag{5.2}$$

Equation 5.2 is more efficient computationally being approximately 400[1] times faster than equation 5.1.

Equation 5.2 was then evaluated over the sets of degrees-of-freedom and χ^2. A *cut-off* was then specified, above which the probabilities were considered. Then the corresponding mass values were plotted.
For most separations, there was no problem in choosing a value, however, in some separations it was not as simple.

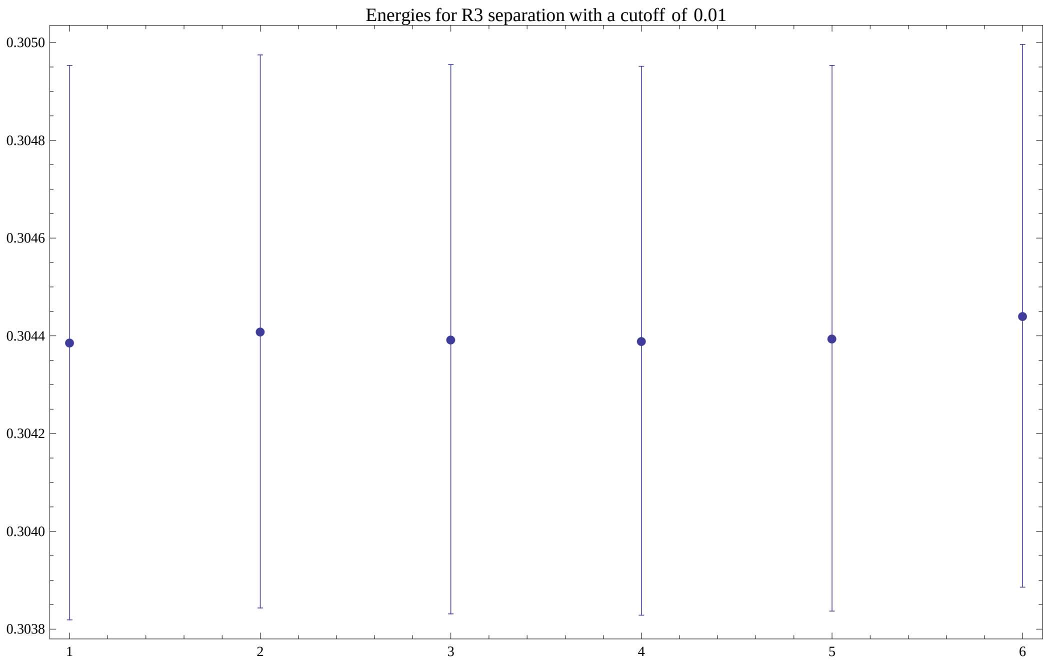

Figure 5.2: Here we may choose any value as they are statistically equivalent.

Figure 5.3 below shows the various values of energy after the "Goodness-of-fit" was applied. This was an interesting outcome as it was not expected. The energy vs. t_{min} was then plotted.

[1]This number was found using *Mathematica's* in-built settings

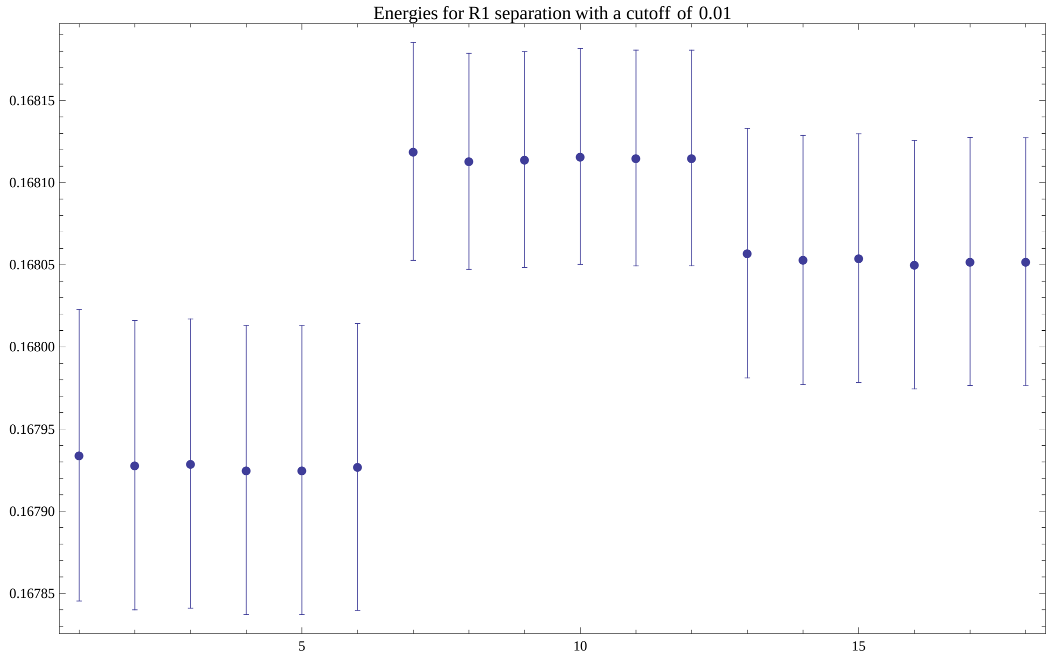

Figure 5.3: Not as simple to choose an appropriate mass value.

Further analysis was performed on the mass values, to determine how to choose appropriate ones.

5.2.1 Mass vs. t_{min}

The mass values were plotted against their corresponding values for the minimum of their fit range, figure 5.4.

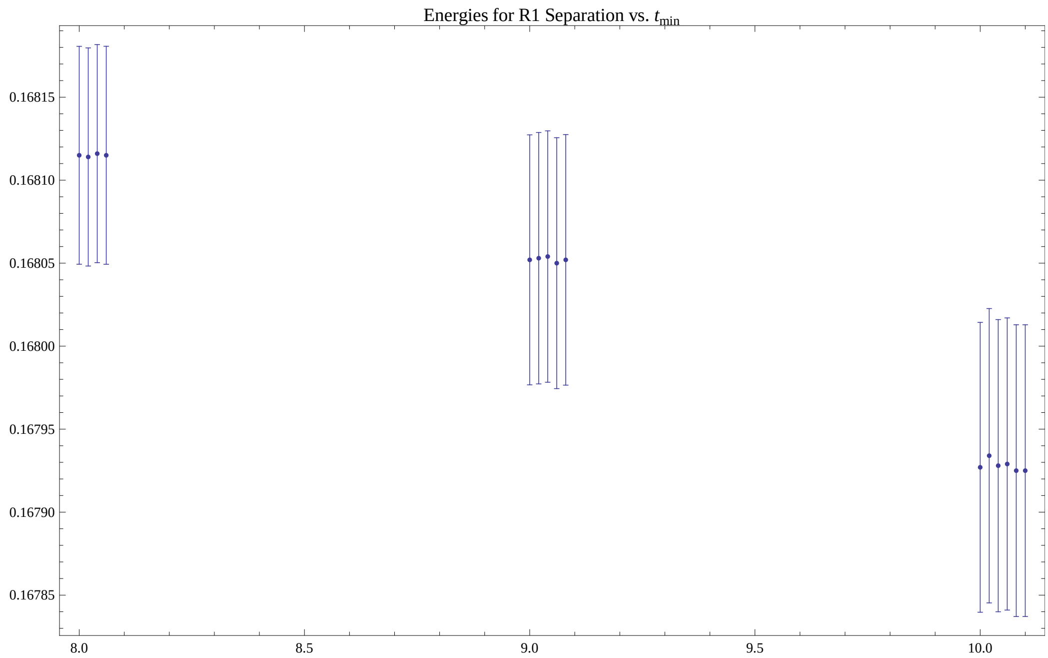

Figure 5.4: The values of mass vs. t_{min} (expanded for clarity).

It was decided that any of the masses from the "smallest mass block" were appropriate to take. The same procedure was performed for the other separations and these masses were plotted with their respective errors, Fig. 5.5.

5.2.2 Some Quantities From R3 Separation

Table 5.1: Various Quantities for 2nd Dataset, 1st mass, R3 Separation with a 0.01 Cut-off

χ^2	Masses (GeV)	Degrees of Freedom	Q Values
2.69082	1.63693 ± 0.00305	4	0.6108
3.0052	1.63705 ± 0.00304	5	0.6992
3.06444	1.63696 ± 0.00302	6	0.8007
3.08076	1.63695 ± 0.00302	7	0.8774
3.08527	1.63698 ± 0.00300	8	0.9289
3.66777	1.63722 ± 0.00299	9	0.9318

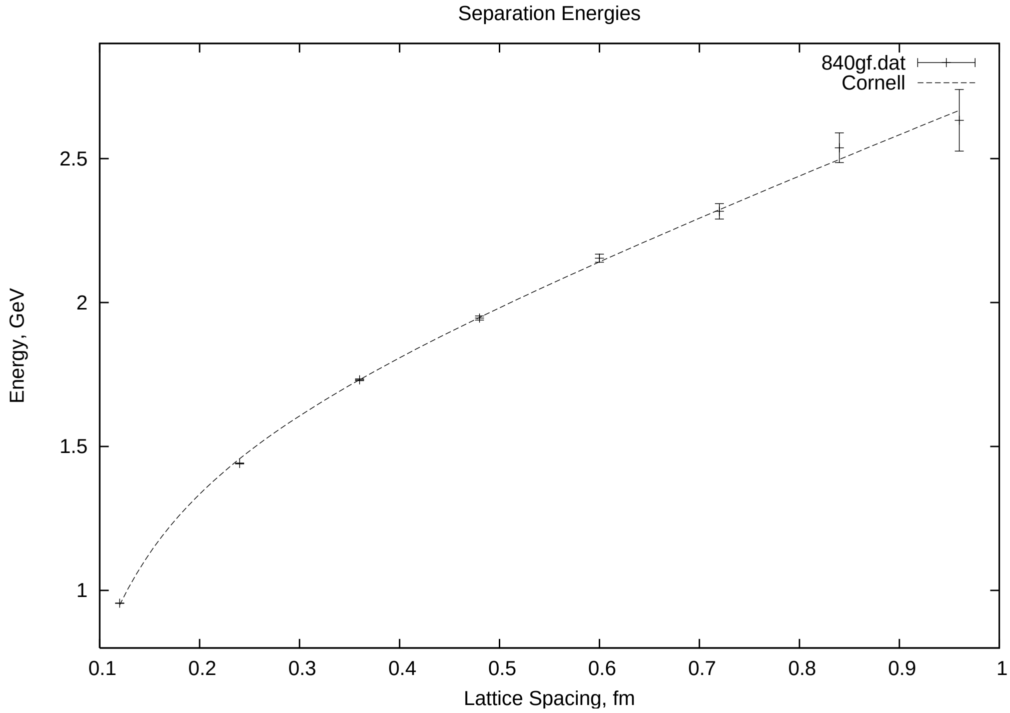

Figure 5.5: $\sqrt{\sigma} = 525.2 \pm 25.6\mathrm{MeV} \qquad \alpha = 0.078 \pm 0.015$

This graph shows the Coulomb part of the interaction ($\alpha = 0.078 \pm 0.015$) over lengths up to about 0.5fm. It also shows the dominance of the linear part (the string tension) over larger distances, i.e. confinement.

Chapter 6

Third Dataset

This dataset used slightly less configurations [6] than the previous analysis. The log plots of the correlation functions for the various separations were all decreasing straight lines, as expected.

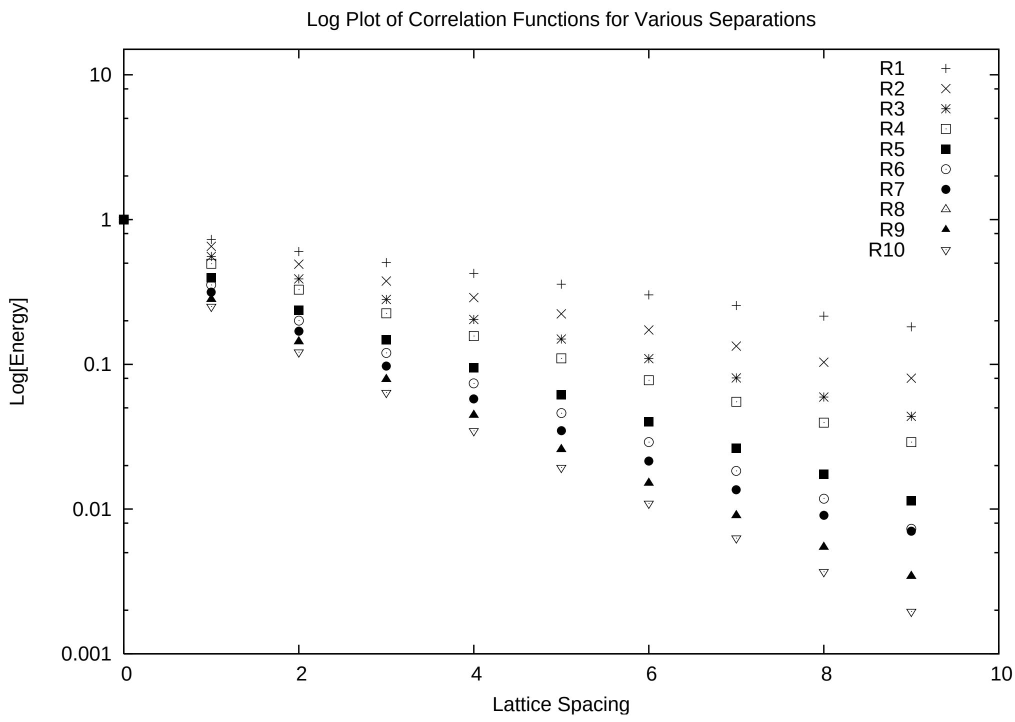

Figure 6.1: Correlation Functions for the 10 separations of the third dataset, all decreasing linearly.

As an example, for the second separation the following data was obtained:

Table 6.1: Various Quantities for 3rd Dataset, R2 Separation with a 0.01 Cut-off

χ^2	Masses (GeV)	Degrees of Freedom	Q Values
11.9871	1.38122 ± 0.00123	4	0.0174
4.04367	1.38112 ± 0.00131	1	0.0443
4.66436	1.38095 ± 0.00130	2	0.0971
8.71435	1.37958 ± 0.00157	3	0.0330
0.05975	1.37901 ± 0.00158	1	0.8069
8.96094	1.37960 ± 0.00157	2	0.0130

The good fit procedure was performed on the data and the filtered energies were plotted against the lattice spacing.

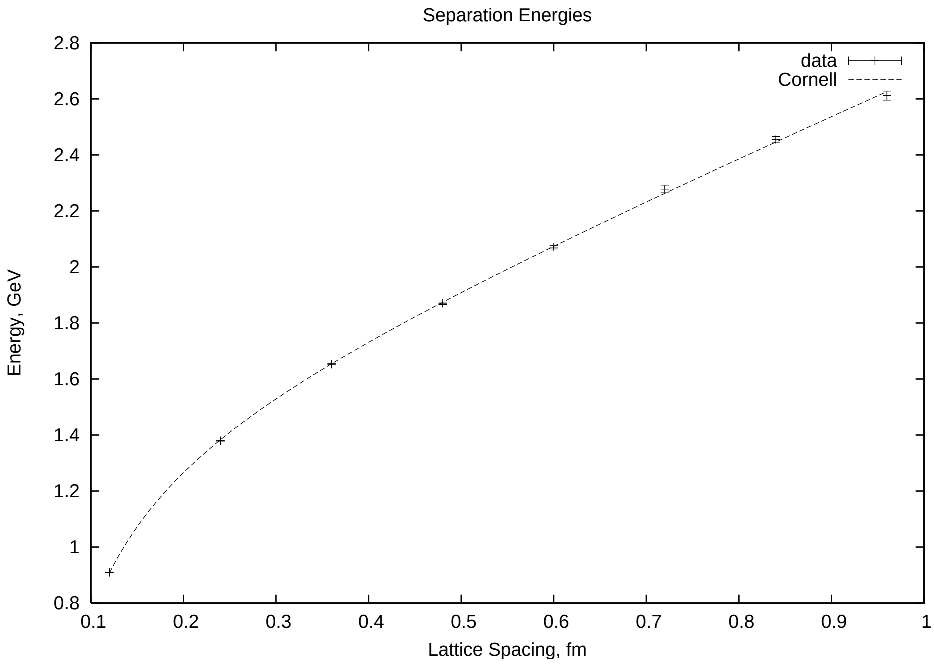

Figure 6.2: A string tension of $\sqrt{\sigma} = 532.6 \pm 19.7\text{MeV}$ was found. $\alpha = 0.071 \pm 0.013$

Chapter 7

Fourth Dataset

A small number of configurations was used for the final analysis [6]. As with the previous datasets, the usual procedure was carried out. That is, the correlation functions were determined and observed to be exponentially decreasing. The energies for each separation were calculated and were then plotted against the lattice spacing.

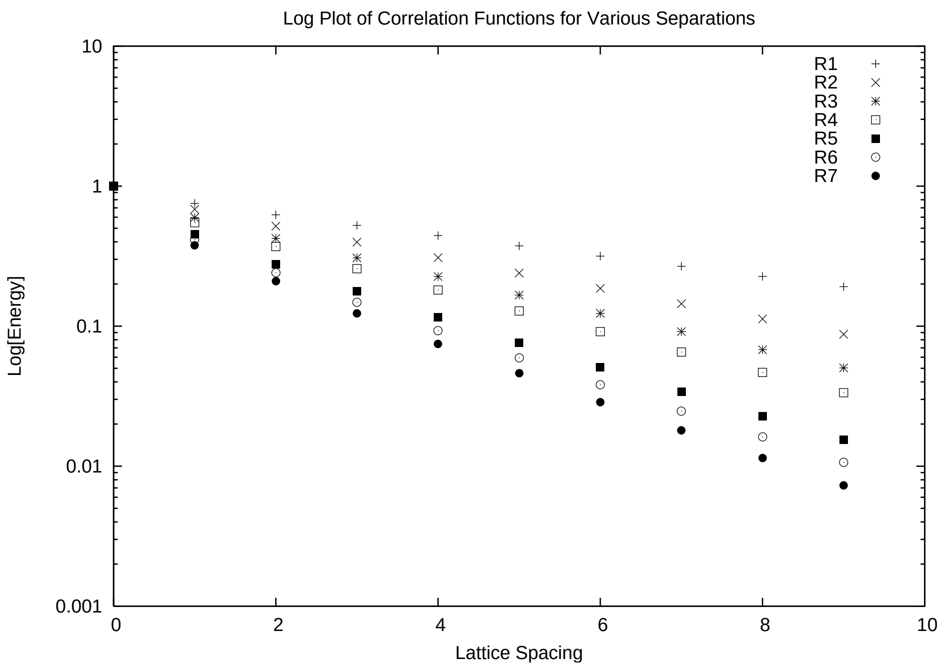

Figure 7.1: Correlation Functions for 7 separations, all decreasing linearly.

Again, the goodness-of-fit function was used to determine the appropriate values to select. The energies were then plotted against the lattice spacing.

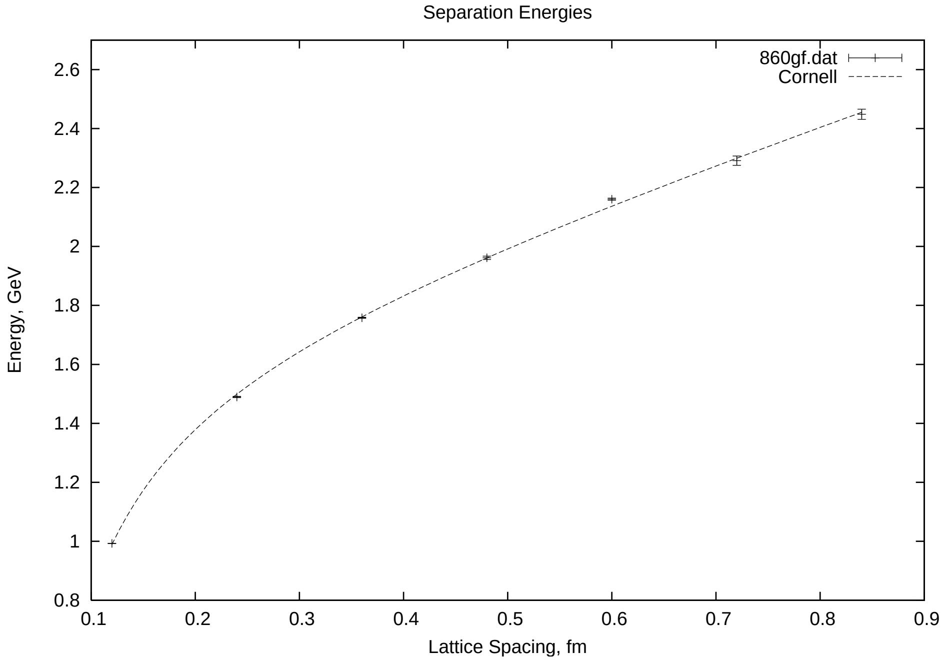

Figure 7.2: A string tension of $\sqrt{\sigma} = 488.2 \pm 22.7$ MeV was found. Coulomb potential parameter, $\alpha = 0.086 \pm 0.014$.

Chapter 8

Results & Conclusions

8.1 String Tension vs. Pion Mass

By plotting the string tensions from the above analyses against the respective pion masses, the string tension for a physical π^+ may be determined by extrapolating the data back to the y-axis via a straight-line fit.

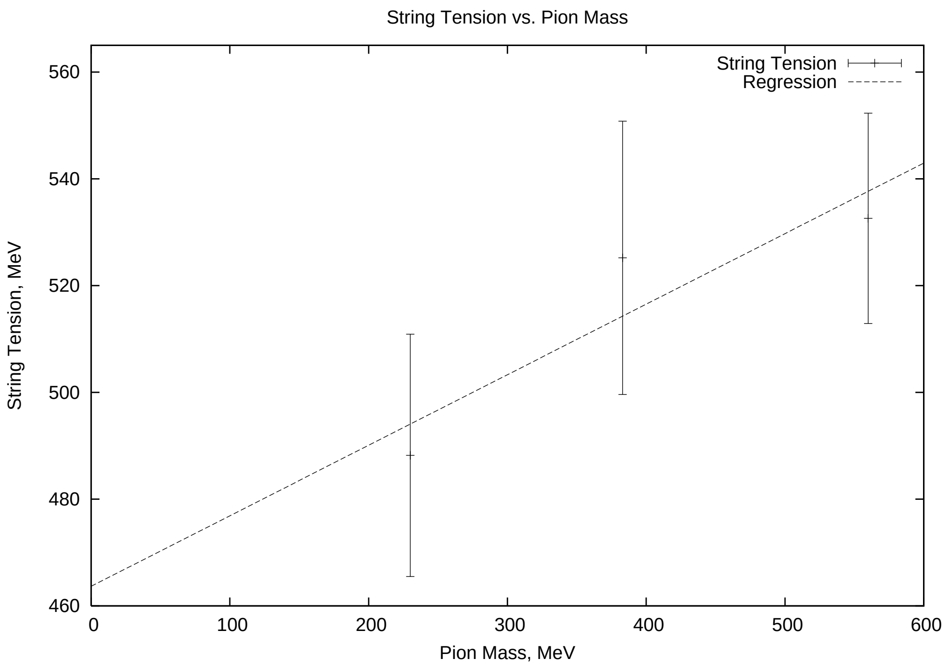

Figure 8.1: The y-intercept is at 463.7 $\pm$ 23.7 MeV.

8.2 α vs. Pion Mass

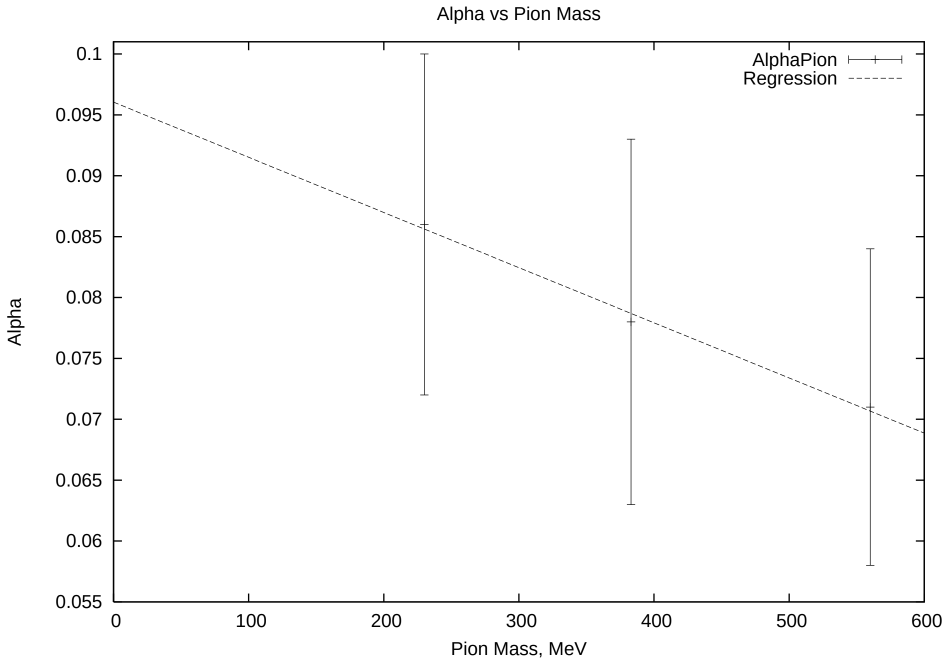

Figure 8.2: The y-intercept is at 0.096 ± 0.002.

The α vs pion mass plot shows that, there too is a mass dependence on the parameter relating to the Coulomb potential. By extrapolating to the y-axis, the value of the Coulomb parameter for a physical pion may be determined.

8.3 Conclusions

This project set out to determine string tensions of static quark-anti-quark pairs. Optimal quantum mechanical operators for the correlation function were calculated by running a series of tests over a range of various values. Then scripts were run on the HPC machines to gather data for the various time and space separations. The data was then imported into *Mathematica* where it was organized and analysed. Functions were defined to make the large datasets more manageable. The data showed that the correlation functions were exponentially decreasing, as expected. The energies for each of the separations were determined using another script which ran χ^2 tests for a goodness-of-fit. The energies for each space separation over several time separations were plotted against lattice spacing. These plots were then fitted via a Cornell potential. The string tensions and Coulomb parameters were then extracted from the Cornell fit. Finally, these values for the three datasets were plotted against their respective pion mass. A mass dependence on both string tension and Coulomb parameter was observed. Values of string tension and Coulomb parameter for a physical π^+ were determined by regression. Further analysis could be carried out with different pion masses to get more accurate values for string tension and Coulomb parameter.

Appendices

Appendix A

Mathematica Notebook

Here I have given an excerpt from one of the *Mathematica* notebooks where I performed my calculations.

Outline

1. Define functions to filter the appropriate data from the datasets.

2. Look at the LogPlots of each separation; they should be linearly decreasing functions.

3. Determine goodness-of-fit by using the "Complete Gamma Function".

   (a) First define the probability function $Q[dof, chi^2]$. For some reason the integral version doesn't work properly with *Mathematica*, so evaluate the indefinite integral first then figure it out at the limits.

   (b) With the probability function, now define the "Goodness of Fit" function with a "cut-off".

   (c) Then find the corresponding chi-squared, mass and error values.

   (d) Use the good fit function and "ErrorListPlot" for each separation to find an appropriate mass to take.

   (e) If it is not clear which one to take then the several mass values for each separation should be plotted. I.e. t_{min} vs mass in order to find the best one.

4. Then, with an energy for each separation plot them all vs lattice spacing.

5. Make a Cornell fit then and determine a string tension.

Setting Directory

SetDirectory[
"C:\\Users\\David\\Dropbox\\Documents\\College\\Dissertation\\Data\\Third Dataset"]

C:\\Users\\David\\Dropbox\\Documents\\College\\Dissertation\\Data\\Third Dataset

Data

Separations

R1 = Import[“R1.dat”];

R2 = Import[“R2.dat”];

R3 = Import[“R3.dat”];

R4 = Import[“R4.dat”];

R5 = Import[“R5.dat”];

R5 = Import[“R6.dat”];

R6 = Import[“R7.dat”];

R7 = Import[“R8.dat”];

R8 = Import["R9.dat"];

R9 = Import["R9.dat"];

R10 = Import["R10.dat"];

Chi-Squared

chiR1 = Import["chiR1.dat"];

chiR2 = Import["chiR2.dat"];

chiR3 = Import["chiR3.dat"];

chiR4 = Import["chiR4.dat"];

chiR5 = Import["chiR5.dat"];

chiR6 = Import["chiR6.dat"];

chiR7 = Import["chiR7.dat"];

chiR8 = Import["chiR8.dat"];

chiR9 = Import["chiR9.dat"];

chiR10 = Import["chiR10.dat"];

chiR11 = Import["chiR11.dat"];

Functions

Needs["ErrorBarPlots`"]

Defining Rows

row[n_, R_]:=Table[R[[n;;;;21]][[i, 2]], {i, 1, 86}]

This function re-organizes each of the “Ri.dat” files such that the time separations are listed together in a “row”. (Imagining for clarity, that for each Ri.dat file the 85 dat files are aligned side-by-side.)
For each separation (i.e. Ri.dat file) all 85 dat files have been concatenated, and each dat file contained data from 0 to 20 time-steps.
I have defined the above function which gives the “row” I mentioned in the first line above.
With this function, I can now manipulate the data much more easily; e.g. averages, errors, etc.

Average value of each row for each separation

```
avg[R1_]:=Table[Table[Mean[row[i, R1]], {i, 1, 21}][[j]], {j, 1, 10}]
```

This function averages each “row” from the row function for each Ri.dat file.
It is this data that we can plot to measure the potential from the correlation function.
Here we are also only plotting up to the first 10 separations since the data gets quite noisy afterwards.

Extracting data from chi-squared files

Define a functions to extract the chi-squared, mass and errors from the chi-squared data:

```
Chi2[chi_]:=Table[chi[[2;;;;3]][[i, 3]], {i, 1, Length[chi[[2;;;;3]]]}]
```

```
Chi2[chiR1]
```

8.97581×10^{8},29040.8,29453.4,1.28498×10^{7},10224.7,3545.55,3574.46,3994.05,

1831.65,933.539,1781.55,1796.73,108.571,29.9442,81.1233,102.656,22.7666,

2.64741,12.978,22.2199,4.10254,5.43901×10^{-18},3.6028,4.07592

```
Mass[chi_]:=Table[chi[[3;;;;3]][[i, 2]], {i, 1, Length[chi[[3;;;;3]]]}]
```

$\mathbf{MassErrors[chi\_]{:=}Table[chi[[3;;;;3]][[\mathit{i},4]],}$

$\mathbf{\{\mathit{i},1,Length[chi[[3;;;;3]]]\}]}$

Degrees of Freedom

$m = t_{\max} - t_{\min} - 1$

m is the number of degrees of freedom. So, define a function which extracts the fit range (i.e. $t_{\max}$ and $t_{\min}$) and computes m.

$\mathbf{dof[chi\_]{:=}(Table[chi[[1;;;;3]][[\mathit{i},5]],\{\mathit{i},1,Length[chi[[2;;;;3]]]\}])-}$

$\mathbf{(Table[chi[[1;;;;3]][[\mathit{i},3]],\{\mathit{i},1,Length[chi[[2;;;;3]]]\}])-1}$

$\mathbf{tmin[R\_]{:=}(Table[\mathit{R}[[1;;;;3]][[\mathit{i},3]],\{\mathit{i},1,Length[\mathit{R}[[2;;;;3]]]\}])}$

Probability Function

$\mathbf{\mathit{Q}[dof\_,fxnchi\_]{:=}\frac{Gamma\left[\frac{dof}{2},\frac{fxnchi}{2}\right]}{Gamma\left[\frac{dof}{2}\right]}}$

Goodness-Of-Fit Function

Define a GOF function where the integral has already been evaluated:

$\mathbf{GOF[chi\_]{:=}\mathit{N}[Table[\mathit{Q}[dof[chi][[\mathit{i}]],Chi2[chi][[\mathit{i}]]],\{\mathit{i},1,Length[dof[chi]]\}],}$

$\mathbf{10]}$

Cutoff Function

$\mathbf{Qcutoff[chi\_,cutoff\_]{:=}ArrayRules[Map[\#Boole[\# > cutoff]\&,GOF[chi]]]}$

Corresponding mass and error values

Now that I have the probabilities of the good fits, I must find the corresponding mass values and their errors

MassGoodFit[chi_, cutoff_]:=

Partition[

Riffle[

Mass[chi][[Flatten[Table[Qcutoff[chi, cutoff][[i]][[1]],

{i, 1, Length[Qcutoff[chi, cutoff]] − 1}], 1]]],

MassErrors[chi][[

Flatten[Table[Qcutoff[chi, cutoff][[i]][[1]],

{i, 1, Length[Qcutoff[chi, cutoff]] − 1}], 1]]]], 2]

ChiGoodFit[chi_, cutoff_]:=

Chi2[chi][[

Flatten[Table[Qcutoff[chi, cutoff][[i]][[1]],

{i, 1, Length[Qcutoff[chi, cutoff]] − 1}], 1]]]

Corresponding chi-squared and dof values

Similarly, definie a funtion that filters out the chi-squareds and dofs.

ChiDof[chi_, cutoff_]:=

Partition[

Riffle[

dof[chi][[Flatten[Table[Qcutoff[chi, cutoff][[i]][[1]],

{i, 1, Length[Qcutoff[chi, cutoff]] − 1}], 1]]],

Chi2[chi][[Flatten[Table[Qcutoff[chi, cutoff][[i]][[1]],

```
{i, 1, Length[Qcutoff[chi, cutoff]] - 1}], 1]]]], 2]
```

Choosing mass values

```
TminMass[chi_, cutoff_]:=
Partition[
Riffle[
tmin[chi][[Flatten[Table[Qcutoff[chi, cutoff][[i]][[1]],
{i, 1, Length[Qcutoff[chi, cutoff]] - 1}], 1]]],
Mass[chi][[Flatten[Table[Qcutoff[chi, cutoff][[i]][[1]],
{i, 1, Length[Qcutoff[chi, cutoff]] - 1}], 1]]]], 2]
```

```
error[chi_, cutoff_]:=
Map[ErrorBar,
MassErrors[chi][[
Flatten[Table[Qcutoff[chi, cutoff][[i]][[1]],
{i, 1, Length[Qcutoff[chi, cutoff]] - 1}], 1]]]]
```

```
tminvsmass[chi_, cutoff_]:=
Partition[Riffle[TminMass[chi, cutoff], error[chi, cutoff]], 2]
```

Analysis

Linear Log plot for correlation function

```
ListLogPlot[avg[R1]]
```

Tried for other separations; no problems.

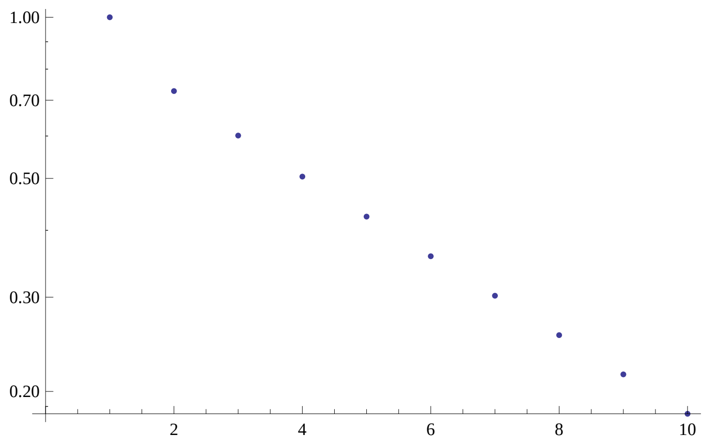

Figure A.1: Log plot of the average of the first separation.

Choosing appropriate mass values

Qcutoff[chiR1, 0.01]

$\{\{18\} \to 0.103719, \{21\} \to 0.250602, \{23\} \to 0.0576823, \{24\} \to 0.130294, \{\_\} \to 0\}$

MassGoodFit[chiR1, 0.01]

{{0.169484,0.0000768359},{0.169127,0.0000807532},{0.169129,0.0000828497}, {0.169124,0.000082548}}

ChiGoodFit[chiR1, 0.01]

$\{2.64741, 4.10254, 3.6028, 4.07592\}$

ErrorListPlot[MassGoodFit[chiR1, 0.01], PlotRange → All]

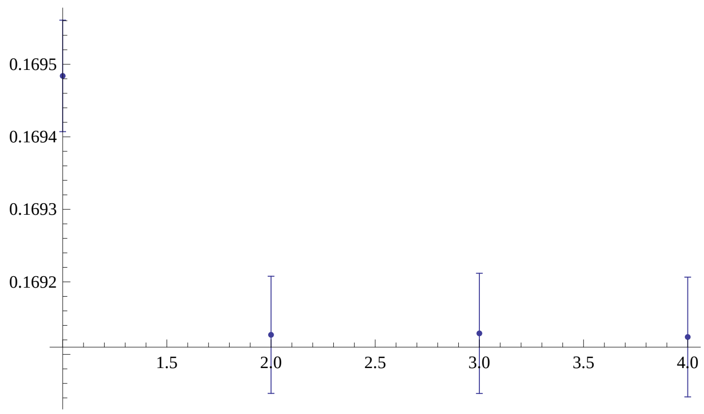

MassGoodFit[chiR3, 0.01]

$\{\{0.11, 6.85679 \times 10^{-15}\}, \{0.308683, 0.000453552\}, \{0.30707, 0.000319915\},$
$\{0.307308, 0.000429126\}, \{0.30743, 0.000415472\}\}$

MassGoodFit[chiR1, 0.01][[3]]

$\{0.169129, 0.0000828497\}$

ErrorListPlot[MassGoodFit[chiR2, 0.01], PlotRange → All]

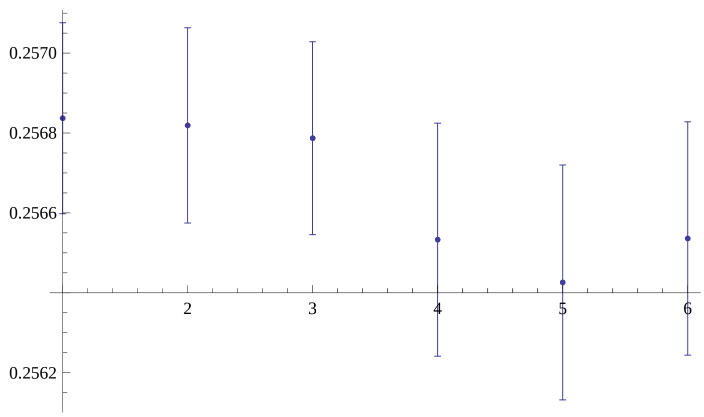

ErrorListPlot[MassGoodFit[chiR3, 0.01]]

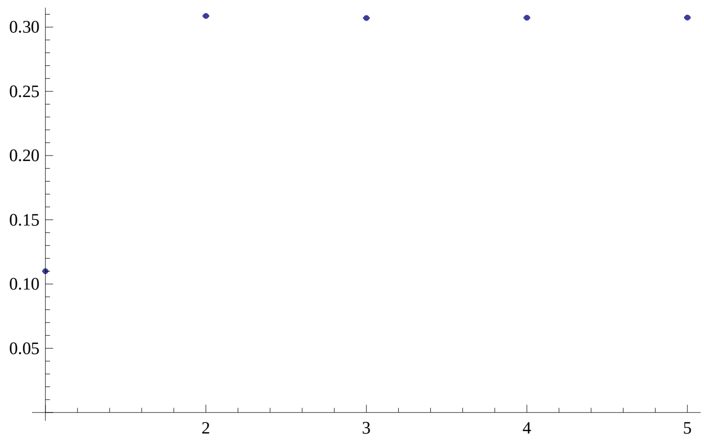

ErrorListPlot[MassGoodFit[chiR4, 0.01]]

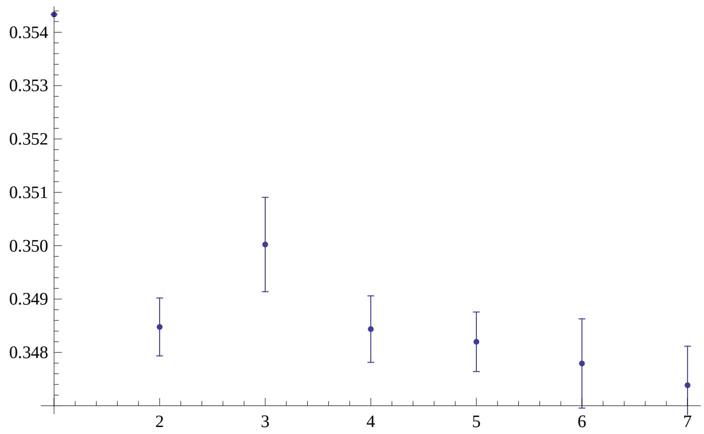

ErrorListPlot[MassGoodFit[chiR5, 0.01]]

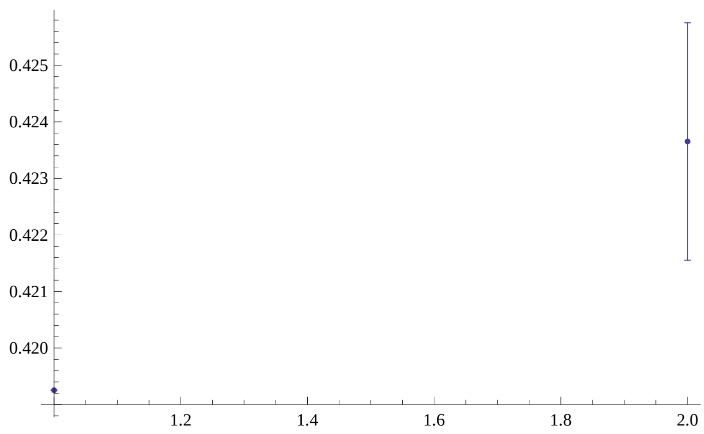

ErrorListPlot[MassGoodFit[chiR6, 0.01]]

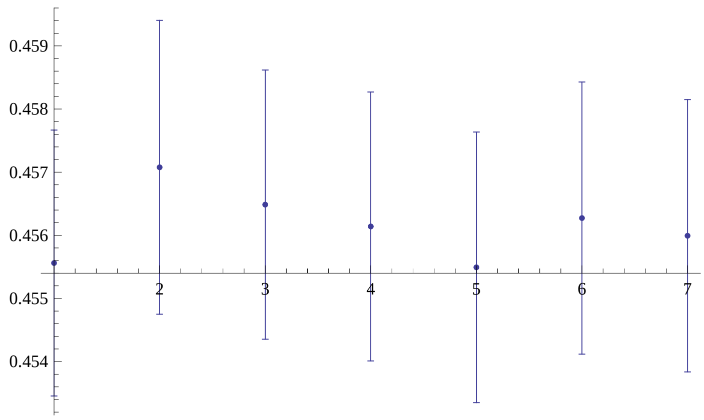

ErrorListPlot[MassGoodFit[chiR7, 0.01], PlotRange → All]

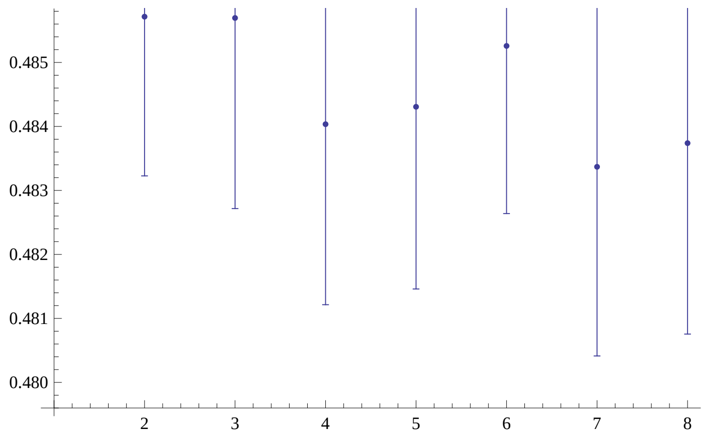

MassGoodFit[chiR7, 0.01][[3]]

$\{0.456486, 0.0021317\}$

ErrorListPlot[MassGoodFit[chiR8, 0.01]]

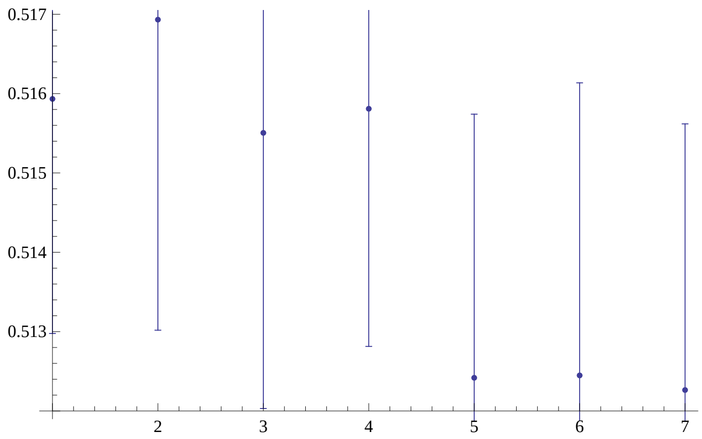

MassGoodFit[chiR8, 0.01][[3]]

$\{0.485695, 0.00297867\}$

ErrorListPlot[MassGoodFit[chiR9, 0.01]]

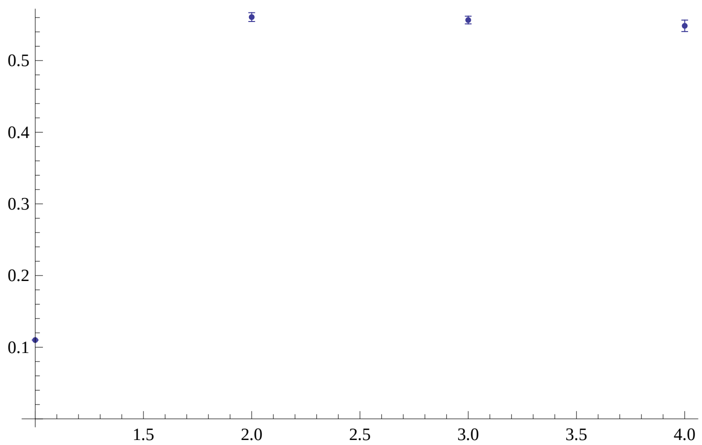

ErrorListPlot[MassGoodFit[chiR10, 0.01]]

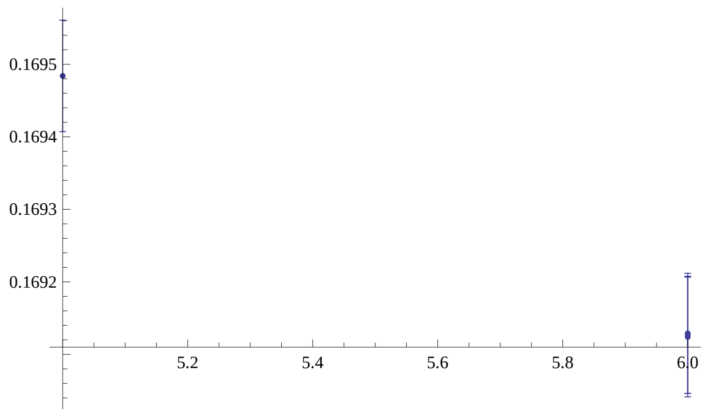

Need to plot mass vs t_{min}

tminvsmass[chiR1, 0.01]

{{{5, 0.169484}, ErrorBar[0.0000768359]}, {{6, 0.169127, },
ErrorBar[0.0000807532]}, {{6, 0.169129}, ErrorBar[0.0000828497]},
{{6, 0.169124}, ErrorBar[0.000082548]}}

ErrorListPlot[tminvsmass[chiR1, 0.01], PlotRange → All]

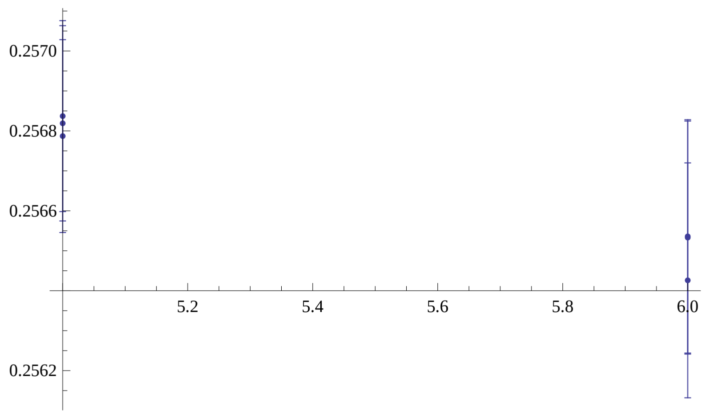

tminvsmass[chiR2, 0.01]

{{{5, 0.256837}, ErrorBar[0.000238976]}, {{5, 0.256819}, ErrorBar[0.000244376]},
{{5, 0.256787}, ErrorBar[0.00024137]}, {{6, 0.256533}, ErrorBar[0.000291634]},

$\{\{6, 0.256426\}, \text{ErrorBar}[0.000293951]\}, \{\{6, 0.256536\}, \text{ErrorBar}[0.000292024]\}\}$

ErrorListPlot[tminvsmass[chiR2, 0.01], PlotRange → All]

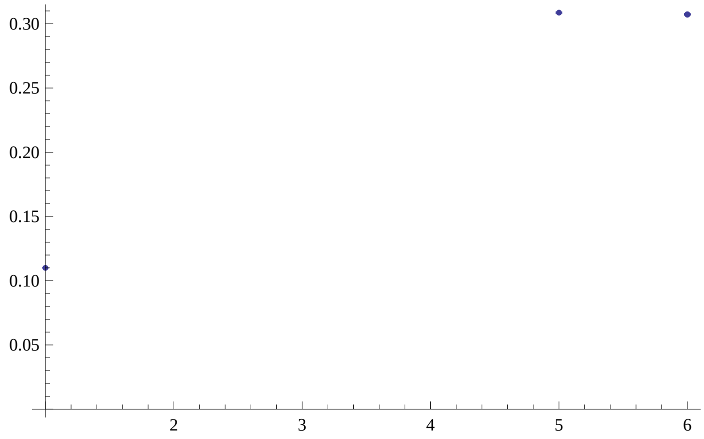

tminvsmass[chiR3, 0.01]

$\{\{\{1, 0.11\}, \text{ErrorBar}[6.85679\times10^{-15}]\}, \{\{5, 0.308683\}, \text{ErrorBar}[0.000453552]\},$

$\{\{6, 0.30707\}, \text{ErrorBar}[0.000319915]\}, \{\{6, 0.307308\}, \text{ErrorBar}[0.000429126]\},$

$\{\{6, 0.30743\}, \text{ErrorBar}[0.000415472]\}\}$

ErrorListPlot[tminvsmass[chiR3, 0.01]]

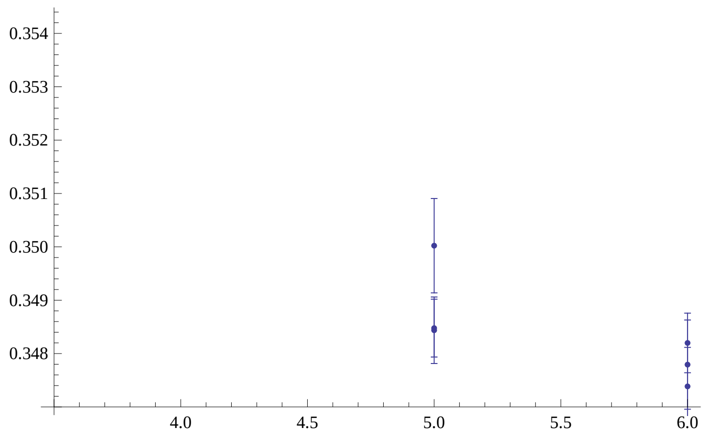

tminvsmass[chiR4, 0.01]

$\{\{\{1, 0.354333\}, \text{ErrorBar}[1.63961\times10^{-12}]\}, \{\{5, 0.348477\}, \text{ErrorBar}[0.000541807]\},$

$\{\{5, 0.350022\}, \text{ErrorBar}[0.000883857]\}, \{\{5, 0.348437\}, \text{ErrorBar}[0.000623277]\},$
$\{\{6, 0.348199\}, \text{ErrorBar}[0.00055809]\}, \{\{6, 0.347793\}, \text{ErrorBar}[0.000836258]\},$
$\{\{6, 0.347385\}, \text{ErrorBar}[0.00073106]\}\}$

ErrorListPlot[tminvsmass[chiR4, 0.01]]

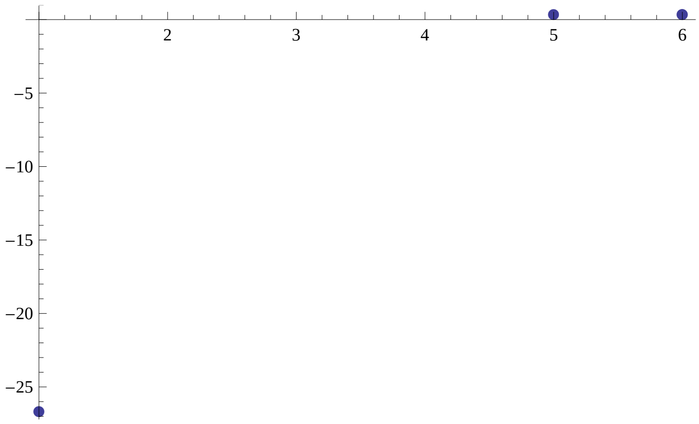

tminvsmass[chiR5, 0.01]

$\{\{\{1, -26.6474\}, \text{ErrorBar}[6.1782\times10^{-12}]\}, \{\{5, 0.387031\}, \text{ErrorBar}[0.00108842]\},$
$\{\{6, 0.385075\}, \text{ErrorBar}[0.0011842]\}, \{\{6, 0.385009\}, \text{ErrorBar}[0.00118191]\}\}$

ErrorListPlot[tminvsmass[chiR5, 0.01]]

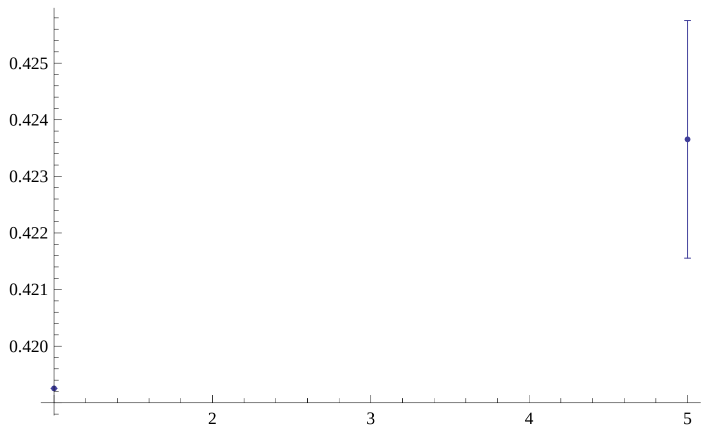

tminvsmass[chiR6, 0.01]

$\{\{\{1, 0.419254\}, \text{ErrorBar}[4.31411\times10^{-12}]\}, \{\{5, 0.423654\}, \text{ErrorBar}[0.00209894]\}\}$

ErrorListPlot[tminvsmass[chiR6, 0.01], PlotRange → All]

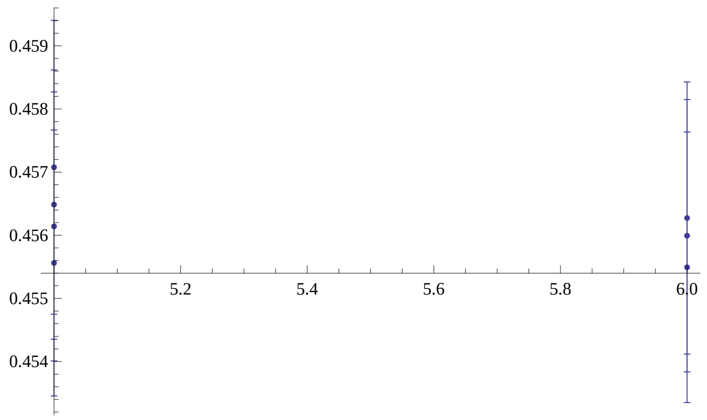

ErrorListPlot[tminvsmass[chiR7, 0.01], PlotRange → All]

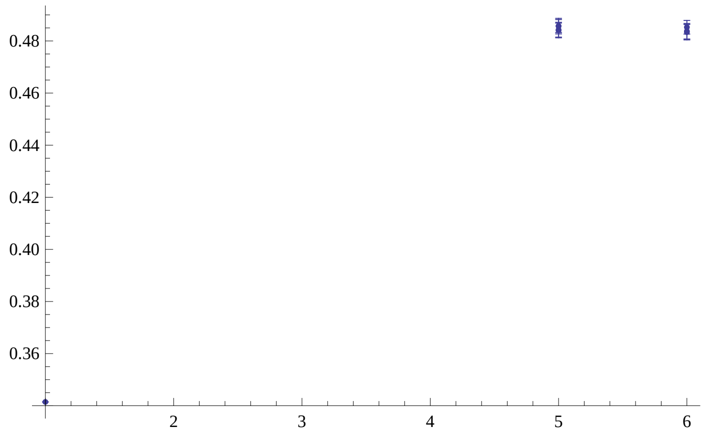

ErrorListPlot[tminvsmass[chiR8, 0.01], PlotRange → All]

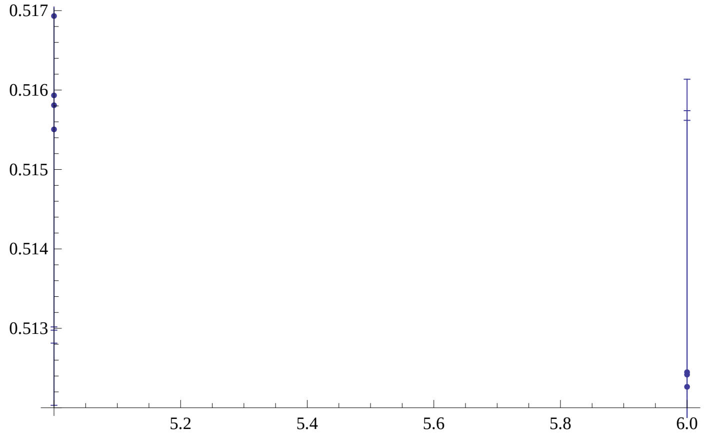

ErrorListPlot[tminvsmass[chiR9, 0.01]]

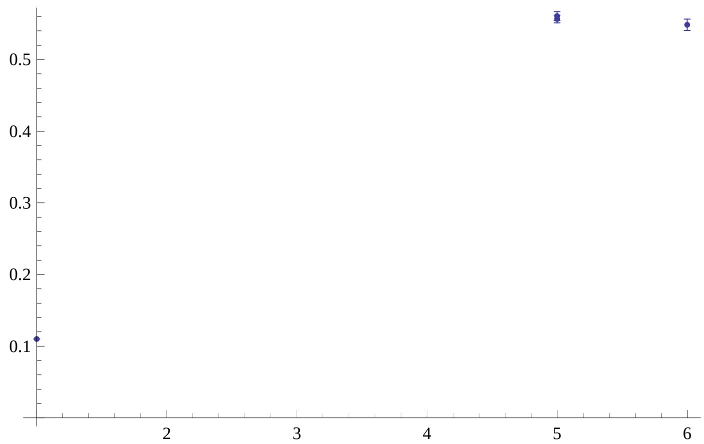

ErrorListPlot[tminvsmass[chiR10, 0.01]]

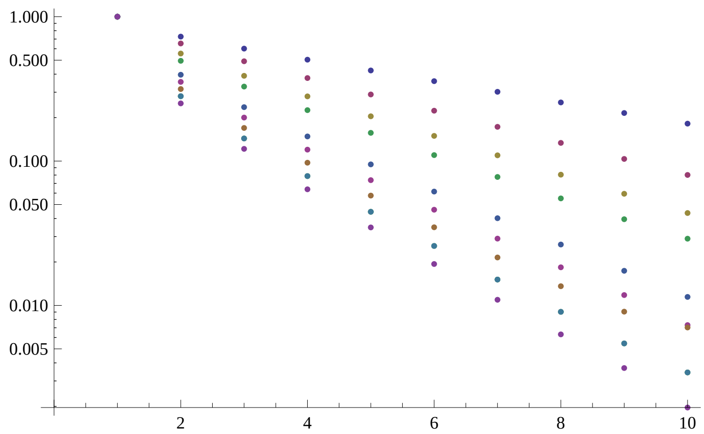

Exporting Data (for Gnuplot)

Export["avgR1.dat", avg[R1]]

avgR1.dat

Export["avgR2.dat", avg[R2]]

avgR2.dat

Export["avgR3.dat", avg[R3]]

avgR3.dat

Export["avgR4.dat", avg[R4]]

avgR4.dat

Export["avgR5.dat", avg[R5]]

avgR5.dat

Export["avgR6.dat", avg[R6]]

avgR6.dat

Export["avgR7.dat", avg[R7]]

avgR7.dat

Export["avgR8.dat", avg[R8]]

avgR8.dat

Export["avgR9.dat", avg[R9]]

avgR9.dat

Export["avgR10.dat", avg[R10]]

avgR10.dat

Fitting

data808gf = {{0.169129, 0.0000828497}, {0.256533, 0.000291634}, {0.307308, 0.000429126}, {0.347793, 0.000836258}, {0.385075, 0.0011842}, {0.423654, 0.00209894}, {0.456486, 0.0021317}, {0.485695, 0.00297867}}

{{0.169129, 0.0000828497}, {0.256533, 0.000291634}, {0.307308, 0.000429126},

{0.347793, 0.000836258}, {0.385075, 0.0011842}, {0.423654, 0.00209894},
{0.456486, 0.0021317}, {0.485695, 0.00297867}}

Partition[
Flatten[Riffle[{0.12, 0.24, 0.36, 0.48, 0.6, 0.72, 0.84, 0.96},
data808gf * 5.3778]], 3]

{{0.12, 0.909542, 0.000445549}, {0.24, 1.37958, 0.00156835},
{0.36, 1.65264, 0.00230775}, {0.48, 1.87036, 0.00449723},
{0.6, 2.07086, 0.00636839}, {0.72, 2.27833, 0.0112877},
{0.84, 2.45489, 0.0114639}, {0.96, 2.61197, 0.0160187}}

Exporting data for Gnuplot.

Export["808gf.dat",
Partition[
Flatten[Riffle[{0.12, 0.24, 0.36, 0.48, 0.6, 0.72, 0.84, 0.96},
data808gf * 5.3778]], 3]]

808gf.dat

Making a Cornell Fit

Table[
Take[
Partition[Flatten[Riffle[{0.12, 0.24, 0.36, 0.48, 0.6, 0.72, 0.84, 0.96},
data808gf * 5.3778]], 3][[*i*]], 2], {*i*, 1, 8}]

{{0.12, 0.909542}, {0.24, 1.37958}, {0.36, 1.65264}, {0.48, 1.87036},
{0.6, 2.07086}, {0.72, 2.27833}, {0.84, 2.45489}, {0.96, 2.61197}}

Fit[

Table[

Take[

Partition[Flatten[Riffle[{0.12, 0.24, 0.36, 0.48, 0.6, 0.72, 0.84, 0.96},

data808gf * 5.3778]], 3][[i]], 2], {i, 1, 8}], $\left\{1, x, \frac{1}{x}\right\}$, x]

$1.352 - \frac{0.071}{x} + 1.44x$

Plots

Log plots of correlation functions.

ListLogPlot[Map[avg, {R1, R2, R3, R4, R5, R6, R7, R8, R9, R10}]]

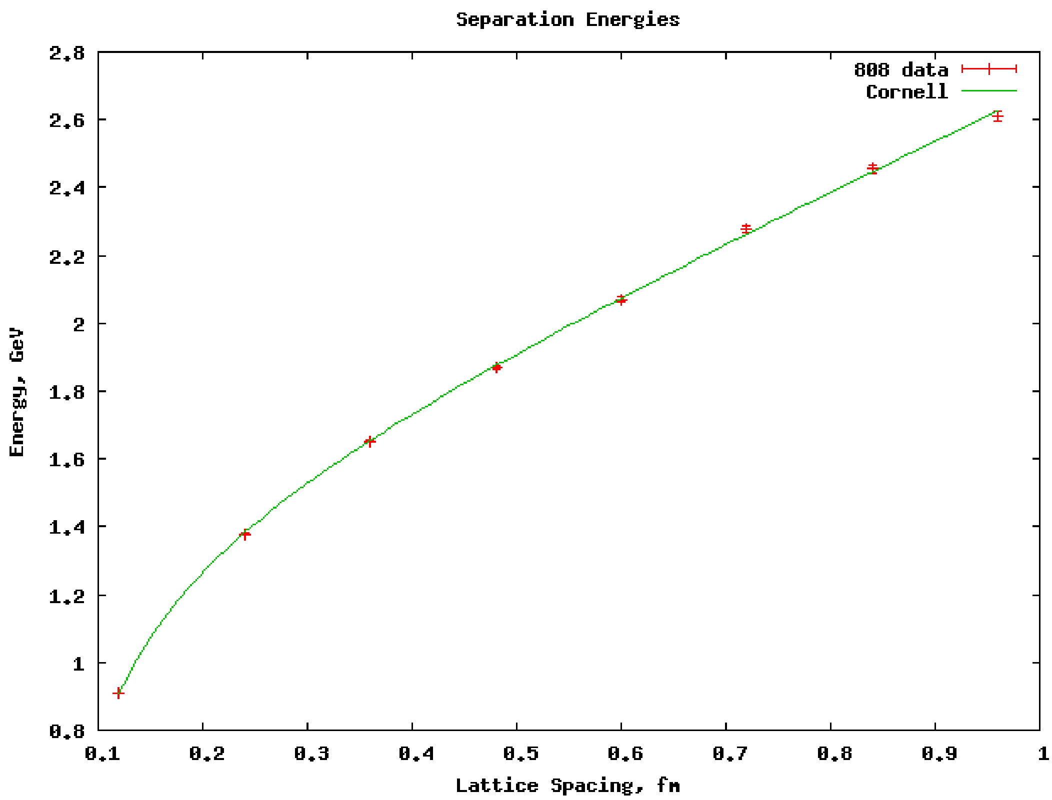

Plotted and fit parameters found using Gnuplot.

$V(r) = V_0 - \frac{\alpha}{r} + \sigma\mathrm{r}$

$V_0 = 1.352$
$\alpha = 0.071$

$\boldsymbol{\sigma = 1.44}$

Results

So string tension in GeV/fm is

$\mathbf{\{1.44, 0.20\}}$

$\{1.44, 0.20\}$

So in $(\mathrm{GeV})^2$

$\mathbf{0.197 * \{1.44, 0.2\}}$

$\{0.28368, 0.0394\}$

so $\sqrt{\sigma}$ in GeV is

$\mathbf{\sqrt{0.28368} \pm 0.5 * 0.0394}$

0.532616 ± 0.0197

Thus in MeV

$0.532616 * 1000 \pm 0.0197 * 1000$

532.616 ± 19.7

so the string tension is:

$$\sqrt{\sigma} = 532.6 \pm 19.7\mathrm{MeV}$$

Bibliography

[1] C. Gattinger and C. B. Lang, "Quantum Chromodynamics on the Lattice: An Introductory Presentation", Springer, 2009

[2] T. Muta, *"Foundations of quantum chromodynamics: an introduction to perturbative methods in gauge theories"* (3rd ed.) World Scientific, 2009

[3] T. DeGrand and C. DeTar, "Lattice Methods for Quantum Chromodynamics", World Scientific, 2006

[4] Press, W., Teukolsky, S., Vetterling, W., Flannery, B., *Numerical recipes in C : the art of scientific computing.* Cambridge University Press, Cambridge, 1992.

[5] C. Morningstar and M. J. Peardon, "Analytic smearing of SU(3) link variables in lattice QCD," Phys. Rev. D **69** (2004) 054501 [hep-lat/0311018].

[6] H. -W. Lin *et al.* [Hadron Spectrum Collaboration], "First results from 2+1 dynamical quark flavors on an anisotropic lattice: Light-hadron spectroscopy and setting the strange-quark mass," Phys. Rev. D **79** (2009) 034502 [arXiv:0810.3588 [hep-lat]].

[7] G. Goldrian, T. Huth, B. Krill, J. Lauritsen, H. Schick, I. Ouda, S. Heybrock, D. Hierl, T. Maurer, N. Meyer, A. Schafer, S. Solbrig, T. Streuer, T. Wettig, D. Pleiter, K. H. Sulanke, F. Winter, H. Simma, S. F. Schifano, R. Tripiccione, A. Nobile, M. Drochner, T. Lippert, Z. Fodor, QPACE: Quantum chromodynamics parallel computing on the cell broadband engine, Comput. Sci. Eng. 10 (2008)

[8] Han, M., and Y. Nambu. "modifying the original integer-changes proposal of Phys." (1965): 1006.

[9] Hooft, GerardusT. "Renormalizable Lagrangians for Massive Yang-Mills Fields." Nuclear Physics B 35.1 (1971): 167-188.

[10] Bardeen, William A., H. Fritzsch, and Murray Gell-Mann. "Light-Cone Current Algebra, 0 Decay and e= e Annihilation." Scale and Conformal Symmetry in Hadron Physics. Wiley and Sons (1973).

[11] Fritzsch, H., and M. Gell-Mann. "Proceedings of the Sixteenth International Conference on High Energy Physics, The University of Chicago and National Accelerator Laboratory, 1972." (1973).

[12] Wilson, Kenneth G. *"Confinement of quarks"* Physical Review D 10.8 (1974): 2445.

[13] Watson, Andrew *"The Quantum Quark"* Cambridge University Press, 2004,